

# Evolution of Muon Alignment with 2010 Data

## 1. Introduction

This document provides estimates of muon alignment resolution in 2010 from all available sources of track-based data. The general plan is to use results from photogrammetry and hardware alignment as a first geometry, update it with 2010 cosmic rays where applicable and beam-halo in the endcap, and then update that with muons from collisions as they become available. To avoid worsening the resolution with track-based statistical errors, chamber alignments would only be updated if they are statistically inconsistent with zero.

Alignment reach with collisions is discussed in detail in Section 2, cosmic rays in Section 3, and beam-halo in Section 4. The document concludes with an Alignment Plan and Milestones (Section 5), which collates these results into a coherent plan with alignment resolution estimates.

## 2. Resolution versus Integrated Luminosity from Collisions

It's important to know how the resolution of the track-based alignment procedure depends on the integrated luminosity of collected data. It allows us to see the reach of the procedure and compare it with other alignment approaches, to plan the future alignment strategy.

The ultimate goal of alignment is to improve the geometry. Before we move a chamber, we should be sure that by moving it, the geometry is strictly improved. If a chamber was crossed by fewer than 5 tracks, we do not align it. If the calculated change in position is more than its uncertainty, we know that the correction would be an improvement, and therefore move the chamber. Conversely, if the correction is consistent with zero, we are not sure whether the geometry will improve or not, so we do not move it. We call this set of rules the chamber motion policy.

In Fig. 1, the dependence of the alignment resolution on the integrated luminosity is shown, with and without this policy. The geometry prior to alignment is Gaussian-distributed with 3 mm sigma for local  $x$ ,  $y$ , and  $z$ , and 3 mrad for local  $\phi_x$ ,  $\phi_y$ , and  $\phi_z$ . Since the prior geometry is worse than the aligned geometry, the chamber motion policy has little influence on the final resolution. If the prior geometry were better than the track-based calculation, the final resolution would simply be that of the prior geometry.

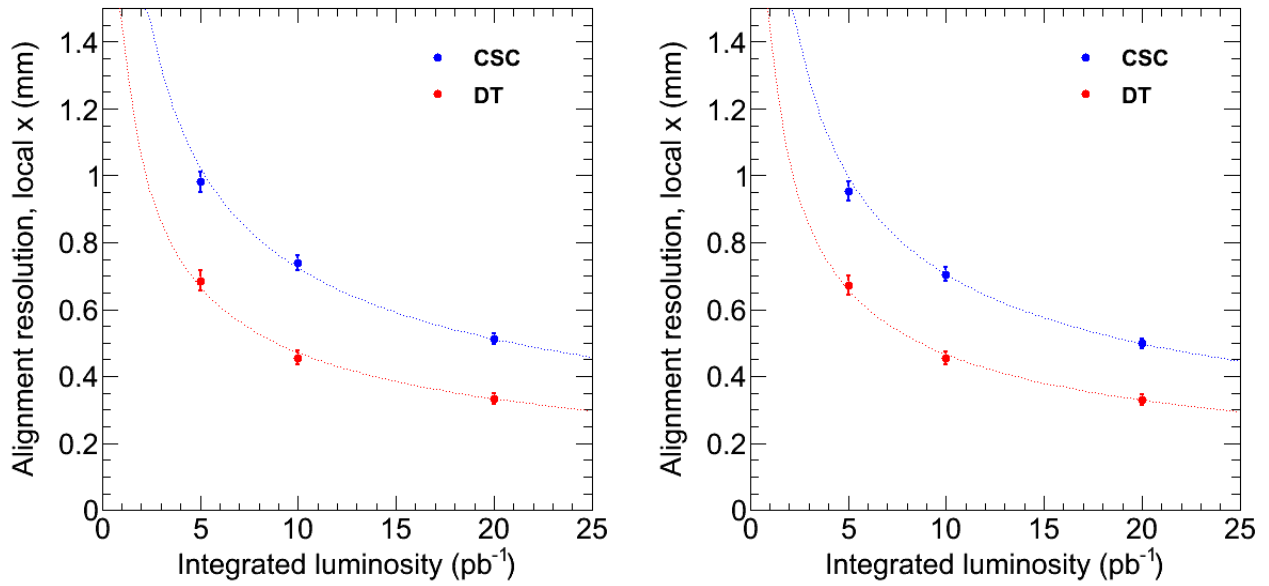


Figure 1: Alignment resolution in the local x direction (global rphi) vs. integrated luminosity with the chamber motion policy (left) and without it (right); the dashed lines are inverse-square-root curves fixed at the 20 pb<sup>-1</sup> points.

In the above study, a Monte Carlo (MC) collisions sample at 7 TeV is used (/InclusiveMu15/Summer09-MC\_31X\_V3\_7TeV\_SD\_Mu9-v1). This sample includes muons from single-quark decays, but not from quarkonia, Drell-Yan, or on-shell W and Z processes. Moreover, muons from cosmic rays are also not included. The sample is divided into three non-overlapping subsamples with integrated luminosities of 5, 10, and 20 pb<sup>-1</sup> to ensure their statistical independence.

Being closest to the tracker, the innermost chambers are expected to have the best resolution. Figure 2 shows the dependence of resolution on integrated luminosity in several groups of inner chambers.

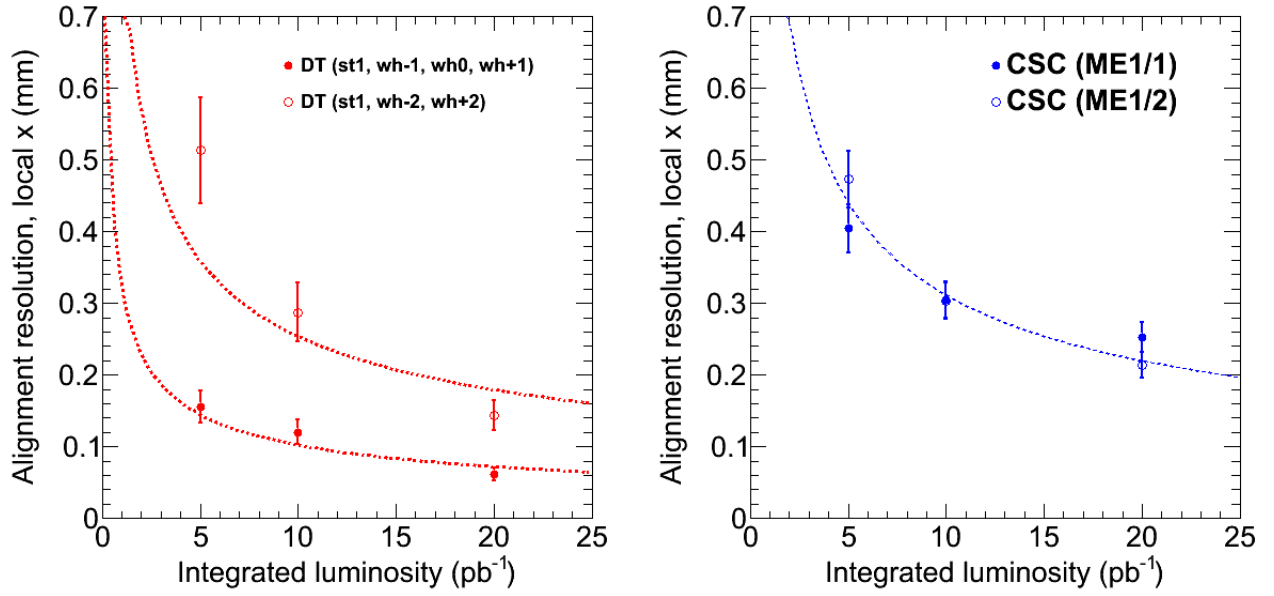


Figure 2: Alignment resolution vs. integrated luminosity for the innermost chambers; dashed lines are inverse-square-root fits. Note that the vertical axis is more zoomed-in than in Fig. 1.

## 2.1 Optimal momentum selection

In the previous section, tracks were required to have  $p_T > 15$  GeV. It was shown [1] that changing the requirement from  $p_T > 20$  GeV to  $p_T > 15$  GeV improved alignment results by 30%. Loosening the cut provided more tracks per chamber without significantly widening the residuals distributions. The optimal cut may be lower than 15 GeV, and the optimum is likely a cut on  $|p|$ , rather than  $p_T$ , especially in the endcaps.

Studies of  $p_T$  cuts are limited by the available MC samples: the sample used to estimate 5, 10, and 20 pb<sup>-1</sup> resolutions is pre-filtered with  $p_T > 15$  GeV at generator level, so looser cuts cannot be tested. A ppMuXLoose sample is available with only a  $p_T > 2.5$  GeV generator level cut, but its total integrated luminosity is only 0.13 pb<sup>-1</sup> and thus the ppMuXLoose results cannot be directly compared with the ppMuX results. Optimization studies with ppMuXLoose are shown in Fig. 3 below.

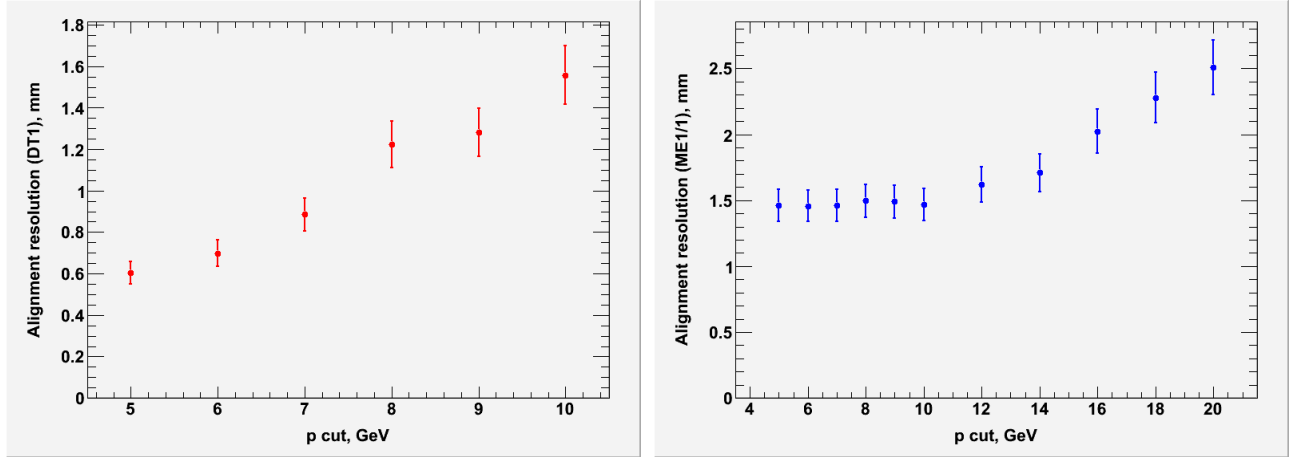


Figure 3: Alignment resolution vs.  $|p|$  cut, first barrel station on left, ME1/1 on the right.

In ME1/1, the  $|p|/p_T$  ratio is about 1/4. The  $p_T > 2.5$  GeV cut in the ppMuXLoose sample is therefore an effective  $|p| > 10$  GeV cut, which explains why all  $|p|$  cuts less than 10 GeV are equivalent. Other than that, there is no observed minimum in alignment resolution vs.  $|p|$  cut: including more tracks is always better.

## 2.2 Limitation from tracker global distortion

Although a local  $x$  resolution of about 1 mm can be achieved with 5 pb<sup>-1</sup> if the tracker is perfectly aligned, muon chamber positions would be less accurate if the tracker is misaligned. The effect of random local variations in tracker module positions is negligible for muon alignments up to 50 pb<sup>-1</sup> [2], but systematic, global distortions of the whole tracker from weak modes of the tracker alignment can be highly relevant.

In the set of tracks that were used for alignment, a global distortion has been observed. This distortion is presented for an example chamber in Fig. 4. Residuals that would be used in muon alignment depend on the momenta of the tracks; this effect cannot be accounted for by any possible misalignment of the muon chambers (which only introduce trends as a function of the other four track parameters). Furthermore, this dependence is the same for positive and negative muons (symmetric in charge), while track-propagation biases such as magnetic field and material budget errors would be opposite for oppositely charged muons (antisymmetric in charge).

CRAFT-09 aligned with  $p_T > 100$  GeV tracks

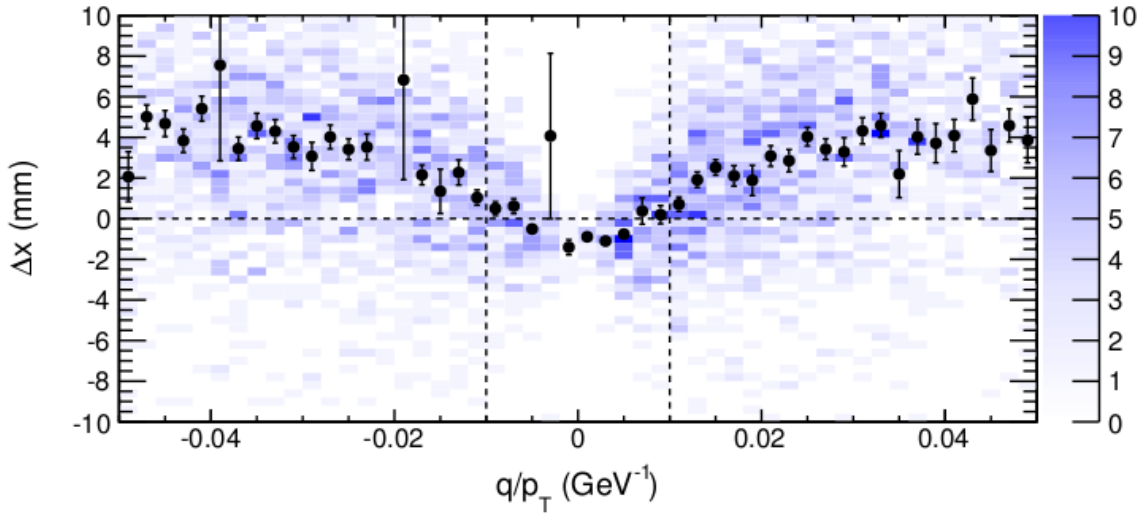


Figure 4: Residuals as a function of momentum expressed as track curvature (charge divided by transverse momentum) in layer 2 of the DT chamber in wheel 0, station 1, sector 10 (directly below the tracker). The color scale is the 2D residuals vs.  $q/p_T$  distribution, points with error bars are average residuals in bins of  $q/p_T$ , and the dashed lines are drawn for guidance. This plot is from CRAFT09, after applying an alignment derived from  $p_T > 100$  GeV tracks.

A study in which the tracker has been globally distorted without affecting the  $\chi^2$  of tracks (and therefore no sensitivity in tracker alignment), can reproduce and even partially cancel this effect [3]. We can therefore conclude that it is most likely due to a similar global distortion of the tracker [4-9], though not the specific mode that has been tested (wrong dependence in  $\phi$ ).

The dependence shown in Fig. 4 leaves open the question of whether low-momentum tracks or high-momentum tracks (or something in between) would yield the correct muon alignment. Assuming that low-momentum tracks are correct would imply that the high-momentum tracks suffer a curvature bias of  $0.5 \text{ TeV}^{-1}$ , and vice-versa. This has been resolved by the measured endpoint of the cosmic ray spectrum in CRAFT08 [10], which shows that the curvature bias is only about  $0.05 \text{ TeV}^{-1}$  in the limit of high momenta, so about 90% of the curvature bias is in low-momentum tracks. This does not lead to large error for physics quantities (a  $0.5 \text{ TeV}^{-1}$  curvature bias affects a 50 GeV track by 0.1%), but it does introduce  $\sim 5$  mm errors into muon alignment. *It is therefore necessary for the tracking bias to be resolved before muon alignments can be performed with low-momentum tracks, such as any muons from collisions.*

### 3. Central Barrel Position Resolution from Cosmic Rays

Alignment of central barrel chambers was demonstrated in CRAFT08 and CRAFT09 using  $p_T > 100$  GeV tracks, and the CRAFT08 results were published in Ref. [11]. In this section, we extrapolate from the Monte Carlo simulations in that document to predict the alignment resolution of existing 2010 cosmic rays.

Cosmic rays only provide large numbers of tracks in chambers directly above and below the tracker, so we only consider DT chambers in wheels -1, 0, and +1, excluding sectors 1 and

7 (on the extreme horizontal sides of CMS). The CRAFT samples had sufficiently large datasets to be systematics-limited at the level of 200 microns in local  $x$  (global  $r\phi$ ). We therefore need to distinguish between "accuracy" and "precision", and use these to quantify the systematic and statistical errors separately.

- Accuracy: ability to reproduce the simulation's true geometry from simulated cosmic rays as an RMS of aligned-minus-true positions after alignment;
- Precision: statistical uncertainty in the alignment, derived by the fitting procedure from the widths and numbers of events in residuals distributions.

The precision of the alignment is simply the statistical error, but the accuracy receives contributions from the statistical error and the systematic error. We will assume that they add in quadrature (that the distribution of systematic errors is Gaussian).

Figure 5 shows the distributions of actual chamber positions relative to the true positions after alignment with a very large 350k cosmic-ray simulation (number of tracks with  $p_T > 100$  GeV). The systematics-limited distributions are roughly Gaussian.

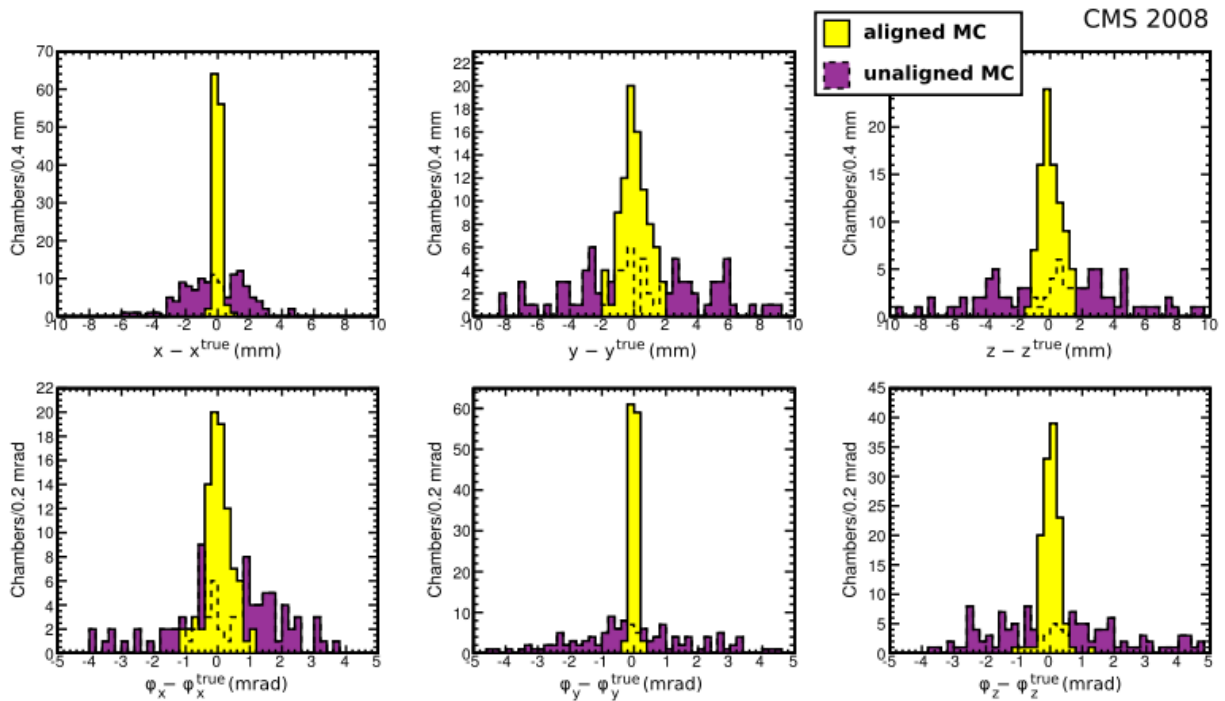


Figure 5: Actual-minus-true positions of all central DT chambers (wheels -1, 0, +1, excluding sectors 1 and 7) for all 6 alignment parameters, using 350k cosmic ray muons with  $p_T > 100$  GeV.

Table 1 shows the accuracy and precision derived from the 350k simulation, a smaller 100k simulation, and extrapolations from 350k to 100k and from 100k to 30k. The 2010 cosmic ray sample has approximately 30k tracks with  $p_T > 100$  GeV, so the 30k extrapolation represents an estimate of alignment accuracy with 2010 cosmic rays. The extrapolation from 350k to 100k allows the reader to compare with the direct 100k simulation, to demonstrate the extrapolation procedure.

|  | <b>x (mm)</b> | <b>y (mm)</b> | <b>z (mm)</b> | <b>phix (mrad)</b> | <b>phiy (mrad)</b> | <b>phiz (mrad)</b> |
|--|---------------|---------------|---------------|--------------------|--------------------|--------------------|
|--|---------------|---------------|---------------|--------------------|--------------------|--------------------|

|   |              |              |              |              |              |              |
|---|--------------|--------------|--------------|--------------|--------------|--------------|
| 350k simulation accuracy                            | 0.192        | 0.841        | 0.630        | 0.417        | 0.095        | 0.287        |
| 350k simulation precision                           | 0.059        | 0.118        | 0.248        | 0.170        | 0.038        | 0.072        |
| prediction of 100k accuracy from 350k extrapolation | 0.213        | 0.861        | 0.742        | 0.496        | 0.112        | 0.309        |
| 100k simulation accuracy                            | 0.209        | 0.889        | 0.836        | 0.497        | 0.148        | 0.303        |
| 100k simulation precision                           | 0.106        | 0.210        | 0.443        | 0.305        | 0.069        | 0.129        |
| prediction of 30k accuracy from 100k extrapolation  | <b>0.264</b> | <b>0.945</b> | <b>1.075</b> | <b>0.681</b> | <b>0.182</b> | <b>0.361</b> |

Table 1: Accuracy (difference from MC truth), precision (statistical uncertainty), and extrapolations from large samples to smaller samples assuming that systematic and statistical errors add in quadrature. The 2010 cosmics dataset has approximately 30k events with  $p_T > 100$  GeV.

The size of the 2010 cosmics dataset is determined by an extrapolation of the whole MuAlGlobalCosmics stream. This stream has 2.5 million globalMuons with  $p_T > 10$  GeV in the range from 126948 (Feb 8, 2010) to 132398 (Mar 29, 2010), and an application of the  $p_T > 100$  GeV requirement would reduce this by a factor of 80 to 30k globalMuons. Therefore, the alignment accuracy in local  $x$  (global  $r_{phi}$ ) is about 0.26 mm.

### 3.1 Merging collisions and cosmic-ray datasets

When the issue with low-momentum tracks is resolved, the optimal alignment strategy will be to combine muons from collisions and cosmic rays, assuming that they are found to be compatible first. Even though the cosmic ray tracks require a special refitting procedure, the two datasets can be combined without difficulty at the level of residuals.

Since a study of alignment from both collisions and cosmic rays hasn't yet been performed, we should conservatively assume that the total alignment uncertainty is the minimum of the alignment uncertainty from non-collisions sources and that from collisions. For cosmic rays in the central barrel (wheels -1, 0, 1, excluding sectors 1 and 7), the turn-over point is about 20 pb-1 (see Fig. 1) assuming (1) that no more cosmic rays are collected, (2) the  $p_T > 100$  GeV cosmic ray cut is not relaxed, and (3) the  $p_T > 15$  GeV collisions cut is not relaxed. Station 1 in particular crosses the same turn-over point at 2 pb-1 (see Fig. 2). The chamber motion policy discussed in Section 2 would allow the alignment of each chamber to be consistently optimized as both collisions and cosmic rays are collected.

## 4. Endcap Chamber Alignment from Beam-Halo

The procedure for aligning CSC chambers with beam-halo muons is sufficiently different from the standard procedure that the two cannot be combined. The beam-halo alignment will therefore only provide a pre-collisions alignment, to be replaced when a more accurate alignment from collisions is available (using the chamber motion policy). The procedure has two steps: the first aligns chambers relative to each other in the same ring using beam-halo muons, and the second aligns the whole rings relative to the tracker using globalMuons from collisions or cosmic rays.

### 4.1 Chambers relative to rings with beam-halo muons

The beam-halo alignment method and results are described in Ref. [11], which shows that a local  $x$  (global  $r\phi$ ) accuracy of 0.27 mm was achieved in 2008 (by comparison with independent photogrammetry). Figure 6 below compares 2010 beam-halo results with photogrammetry for all complete inner rings. (A ring of chambers is "complete" if data could be collected in all chambers; see Ref. [12]).

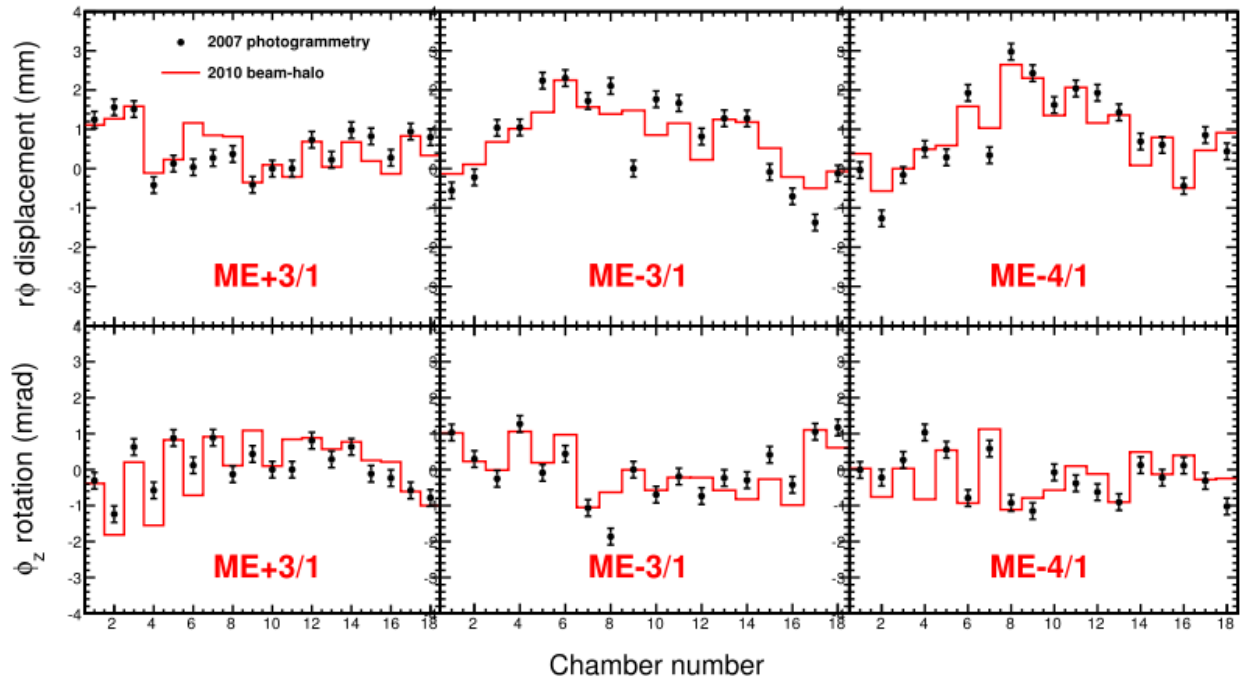


Figure 6: Overlay of 2010 beam-halo (red line) and photogrammetry (points with error bars), relative to ideal geometry, for all complete rings (ME+3/1, ME-3/1, and ME-4/1). The top row shows displacements (local  $x$ /global  $r\phi$ ) and the bottom row shows  $\phi_z$  rotation angles.

It should be noted that these measurements are only relative to the other chambers in the same ring, not necessarily the tracker's coordinate system. To relate the aligned CSC rings to the tracker, we will need to use globalMuons.



## 4.2 Rings relative to tracker with cosmic rays or collisions muons

To align endcap rings as rigid bodies, hit residuals from all chambers in the ring are combined into a single three-parameter fit, where the fit parameters are identified with global  $x$ ,  $y$ , and  $\phi$  corrections to the ring position. An example is shown in Fig 7.

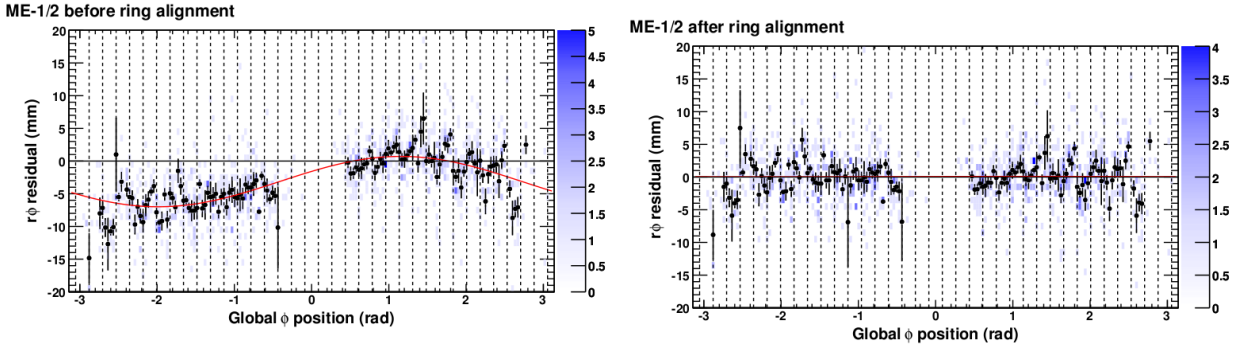


Figure 7: Residuals vs.  $\phi$  of CSC hits before (left) and after (right) ring alignment from CRAFT09 data. The color scale is the 2D residuals vs.  $\phi$  distribution, points with error bars are mean residual vs.  $\phi$ , and the curve is an  $A \sin(\phi) + B \cos(\phi) + C$  fit. The constants  $A$ ,  $B$ , and  $C$ , correspond to global  $x$ ,  $y$ , and  $\phi$  corrections to the ring position.

This procedure can be performed with either collisions or cosmic rays. With simulated collisions, the  $x$ - $y$  and  $\phi$  resolutions are given in Fig. 8. If the 2010 cosmic ray dataset includes hits in both the top and bottom halves of CMS (depends on CSC trigger parameters; true for CRAFT09 but not for CRAFT08), then the cosmic ray alignment will dominate the precision. Ref. [13] shows statistical precisions of ring alignments with CRAFT09, which were typically 0.1 mm in  $x$ , 0.2 mm in  $y$ , and 0.05 mrad in  $\phi$ . The uncertainty in the global  $\phi$  of the ring times its radius is the uncertainty in local  $x$  (global  $r\phi$ ); a 0.05 mrad  $\phi$  uncertainty is a 0.1-0.25 mm local  $x$  uncertainty. Ring alignment parameters from 2010 cosmic rays should be about twice as uncertain, but that makes them equivalent to about 20+ pb $^{-1}$ . The 2010 ring alignment will therefore be performed with cosmic rays, assuming that the trigger conditions were favorable.

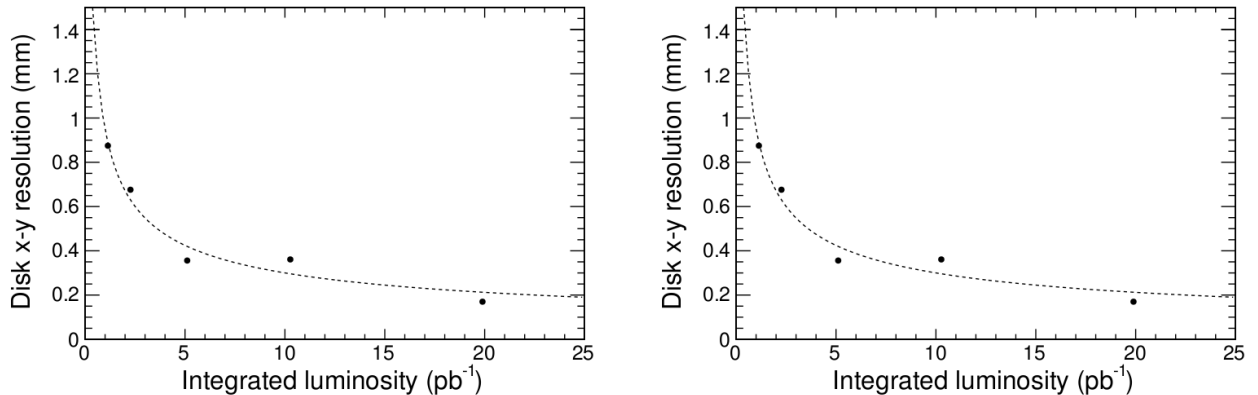


Figure 8: Accuracy of ring alignment procedure as a function of integrated luminosity from simulated collisions only.

The turn-over point, where the alignment of chambers directly relative to the tracker outperforms beam-halo alignment plus whole-ring alignment, is at 20+ pb<sup>-1</sup> when considering all CSC chambers (Fig. 1), but about 15 pb<sup>-1</sup> for ME1/1 and ME1/2 (Fig. 2), assuming a pT > 15 GeV cut for the standard alignment and no more cosmic rays.

### 4.3 Updates to the beam-halo alignment procedure

The principle weakness of the beam-halo procedure, as it is currently defined, is that it requires data from all chambers in the ring. For the 2010 beam-halo dataset, this means that only four rings could be aligned: ME+3/1, ME-3/1, ME-4/1, and ME-3/2. We are currently updating the procedure to include external constraints, such as photogrammetry, in the alignment fit. The combined fit will then solve both the external constraints and the track-based alignment simultaneously, which would fill in data from missing chambers in a globally consistent way.

Another problem that is being investigated is the lack of closure of the complete rings: the sum of pairwise residuals around the 18 or 36-chamber rings is 9 mm, rather than zero. This problem was not present in 2008 beam-halo data, which had no magnetic field. The closure issue could be related to a 1.4 mm change in ring radius when the disk bows in the magnetic field (numerically plausible; must be tested).

## 5. Alignment Plan and Milestones

The first two steps, beyond the initial photogrammetry/hardware alignments, will be to update the central barrel with cosmic rays and the endcap with beam-halo data. Work on these two projects is being done in parallel. To gauge the effect of recent improvements to the Reference-Target procedure [1], Aysen Tatarinov is aligning the 2009 and 2010 cosmic rays with a single updated algorithm. Meanwhile, Jim Pivarski is integrating external constraints into the beam-halo procedure, so that all endcap rings can be aligned.

- Resolution expected from 2010 cosmic rays: 0.26 mm (in local x/global rphi);
- Resolution expected from 2010 beam-halo: 0.27 mm relative to rings;
- Systematic uncertainty in endcap ring positions from cosmic rays: 0.2-0.5 mm (adds to the above in quadrature).

The next step would be to align with low-momentum collisions muons, but this only makes sense (< 5 mm errors) if the global distortion observed in the tracker track sample has been resolved. The most likely solution to this is a  $\chi^2$ -invariant global correction to the tracker shape. We can provide feedback on trial corrections.

Assuming that the global distortion problem has been solved, we can begin aligning chambers relative to the tracker with as few as 2 pb<sup>-1</sup>. Very few chambers would be improved by such a small dataset--- primarily chambers in the innermost stations--- but only the statistically significant corrections would be applied. As data accumulate, more chambers become precise enough for alignment, until nearly all chambers are aligned by the standard algorithm at 20+ pb<sup>-1</sup>. Lower momentum cuts than the current default (pT > 15 GeV) may lead to earlier turn-over points, but the current state-of-the-art is Fig. 1 and 2.

## References

- [1] A. Tatarinov, *Improvements to Track-Based Muon Alignment*, <http://indico.cern.ch/contributionDisplay.py?contribId=1&confId=83944> (Mar 22, 2010).
- [2] J. Pivarski, *50 pb-1 Misalignment Scenario*, <http://indico.cern.ch/contributionDisplay.py?contribId=4&sessionId=0&confId=64775> (Sep 18, 2009).
- [3] M. Stoye, *Constraining Weak Modes with External Information*, <http://indico.cern.ch/subContributionDisplay.py?subContId=1&contribId=10&sessionId=6&confId=76877> (Feb 2, 2010).
- [4-9] Talks related to limitation from tracker global distortion
  - J. Pivarski, *Update on Global Alignment of the Muon System*, <http://indico.cern.ch/contributionDisplay.py?contribId=3&confId=55713> (May 11, 2009).
  - J. Pivarski, *Diagnosing Tracker Weak Modes using Muon Chambers*, <http://indico.cern.ch/contributionDisplay.py?contribId=20&sessionId=0&confId=63612> (Nov 5, 2009).
  - J. Pivarski, *Track-based vs. HW-based DT Alignment Studies*, <http://indico.cern.ch/contributionDisplay.py?contribId=4&confId=75978> (Dec 4, 2009).
  - J. Pivarski, *Relative Alignment of Tracker and Muon System*, <http://indico.cern.ch/subContributionDisplay.py?subContId=1&contribId=54&sessionId=1&confId=75710> (Dec 7, 2009).
  - J. Pivarski, *Global Distortions in CMS Alignment*, <http://indico.cern.ch/contributionDisplay.py?contribId=1&confId=87850> (Mar 11, 2010).
  - J. Pivarski, *Global Distortions in CMS Alignment Revisited*, <http://indico.cern.ch/contributionDisplay.py?contribId=1&confId=87850> (Mar 18, 2010).
- [10] I. Furic, *Momentum Scale in Charge Ratio Analysis*, <http://indico.cern.ch/contributionDisplay.py?contribId=4&confId=87850> (Mar 18, 2010).
- [11] CMS Collaboration, *Alignment of the CMS muon system with cosmic-ray and beam-halo muons*, [2010 JINST 5 T03020](https://arxiv.org/abs/2010.JINST.5.T03020).
- [12] J. Pivarski, *2010 Ring Alignment with Beam-Halo Overlapping Muon Tracks*, <http://indico.cern.ch/contributionDisplay.py?contribId=8&confId=88294> (Mar 19, 2010).
- [13] J. Pivarski, *Alignment Update*, <http://indico.cern.ch/contributionDisplay.py?contribId=1&confId=71857> (Oct 27, 2009).